NACA RM E56A16

NACA

RESEARCH MEMORANDUM

INTERACTION OF AN EXHAUST JET AND ELEMENTARY CONTOURED SURFACES LOCATED IN A SUPERSONIC AIR STREAM

By Joseph F. Wasserbauer and Gerald W. Englert

Lewis Flight Propulsion Laboratory
Cleveland, Ohio

NATIONAL ADVISORY COMMITTEE FOR AERONAUTICS

WASHINGTON

April 6, 1956

Declassified January 20, 1958

NATIONAL ADVISORY COMMITTEE FOR AERONAUTICS

RESEARCH MEMORANDUM

INTERACTION OF AN EXHAUST JET AND ELEMENTARY CONTOURED SURFACES LOCATED IN A SUPERSONIC AIR STREAM

By Joseph F. Wasserbauer and Gerald W. Englert

SUMMARY

The interaction of an exhaust jet and elementary contoured surfaces was studied systematically at a free-stream Mach number of 1.6 over a range of nozzle pressure ratios from a jet-off condition to a pressure ratio of 9. The effect of the presence of streamline fairings between the surfaces and parabolic afterbody housing the exhaust nozzle on this interaction was also investigated. These surfaces were located at two fixed distances from the nozzle centerline.

The interferences from the jet and afterbody tended to raise the average pressure on these surfaces, and the net resultant normal forces thus repelled the surfaces away from the nozzle centerline. With no fairings present, varying the angle on the wedge-type surfaces, varying the radius of curvature on convex-type surfaces, and changing the arc length on the concave-type surfaces had a noticeable effect on normal-force coefficient. Addition of streamlined fairings increased the repelling magnitude of the normal force on the convex- and wedge-type surfaces and shifted the center-of-pressure location toward the nozzle exit.

INTRODUCTION

Several studies have emphasized the problem of the jet effect on aerodynamic surfaces located near the exhaust region of an engine (refs. 1 to 5). Recent studies of the interaction of a jet and a flat surface (refs. 6 to 9) have indicated that the boattail and jet shocks from an engine pod may have considerable effect on wing and tail surfaces.

This report is an extension of the flat-plate study (ref. 6) to include contoured surfaces. Systematic study of jet interaction with various shaped surfaces may lead to better understanding of the more complex cases of jet interaction with various nearby components of the airframe. Families of convex-, concave-, and wedge-type surfaces with and without fairings were studied in the region of an exhaust jet. Data

were taken to determine how the radius of curvature, arc length, and wedge angle for the various surfaces affected normal force, center of pressure, and pressure pulsations. This study was made at a Mach number of 1.6 in the NACA Lewis 8- by 6-foot supersonic wind tunnel over a range of nozzle pressure ratios.

SYMBOLS

A nozzle-exit area, 0.0898 sq ft

C_p pressure coefficient, $\frac{p - p_\infty}{q_\infty}$

L length of surface from nozzle-exit station to surface trailing-edge station

l distance to center of pressure from nozzle-exit station along surface of plate in x-direction

M Mach number

N force normal to x,z-plane, positive when directed toward nozzle centerline

P total pressure at nozzle entrance

p static pressure

q dynamic pressure

r radius

S axial distance from nozzle-entrance station

V velocity

x distance downstream of nozzle-exit station and parallel to free-stream direction

Y distance between nozzle centerline and surface middle chord measured in y-direction

y coordinate orthogonal to x and z coordinates

z spanwise distance from plane of symmetry that passes through nozzle centerline and surface middle chord

Subscripts:

a afterbody

e nozzle exit

j condition in jet when expanded isentropically and one-dimensionally over P/p_∞

n nozzle

∞ free stream

APPARATUS AND PROCEDURE

The jet was supplied by the exit model apparatus reported in reference 10. The exhaust nozzle and one of the convex surfaces without fairing can be seen in the photograph of figure 1(a). The general layout of this model as well as the support system for the various surfaces is shown in figure 1(b). The dimensions of the surfaces, convergent exit nozzle, and parabolic afterbody are given in figure 2.

All surfaces studied were of rectangular plan form and had the same length. The survey station locations are shown on the cross-sectional views of the surfaces in figure 2. Dynamic-pressure pickups were located 2 inches from the surface centerline measured along the surface on all configurations except the 60° arc, which had its pickups 1.058 inches from the surface centerline. The pressure-recording system used with the dynamic pickups was accurate to 100 cycles per second. The middle chords of the surfaces were positioned at vertical distances of 1.4 and 2.03 nozzle-exit radii r_e from the nozzle centerline. The 120° wedge surface and the convex surface having a radius of $2r_e$ were studied with biconvex circular-arc fairings attaching them to the boattail of the jet-exit model. The fairings (fig. 3) had sharp trailing edges and fineness ratios of 3. No fairing was used for the concave surface. However, some data were obtained with this surface extended forward to meet the model afterbody at a distance Y of $1.4r_e$ (fig. 3).

Pressure inside the nozzle was varied from the jet-off value to values producing a jet pressure ratio of 9. Free-stream Mach number was set at 1.6.

RESULTS AND DISCUSSION

Normal-force coefficients and center-of-pressure locations were determined from surface static-pressure distributions. Normal-force

coefficient was arbitrarily considered positive when acting from the surface toward the nozzle centerline. The interferences from the jet and model afterbody in this investigation were such that the net resultant forces always tended to repel the surfaces, and, therefore, the normal-force coefficient was plotted in a negative direction. Also, normal-force coefficient is referenced to nozzle-exit area for all surfaces.

Wedge-Type Surfaces

As the angle of the wedge-type surfaces was decreased, the absolute value of the normal-force coefficient also decreased (fig. 4). Trigonometric relations show that the normal force varies as the sine of half the wedge angle if the pressures on the surface are assumed invariant with wedge angle. However, at vertical distances between plate and nozzle centerline of Y/r_e equal to 1.4 and 2.03, the data indicate that the absolute values of the normal-force coefficient are generally slightly lower than would be given by this relation, indicating that the average pressure on the wedge surface decreased with decreasing angle. This general trend can be explained by the pressure profiles of figure 5. This figure shows that the pressures downstream of the boattail shock are appreciably increased. As the angle of the surface decreases, the line of intersection of the boattail shock with the surfaces is swept rearward. As the line of intersection is swept rearward, less surface is exposed to the high pressure regions behind the shocks, thereby decreasing the absolute value of the normal-force coefficient (fig. 4(a)).

Center-of-pressure location was generally shifted farther downstream of the nozzle exit as the angle of the surface was decreased (fig. 4(a)). This shift may also be caused by the rearward movement of the intersection of the boattail and jet shocks as explained previously.

With fairings present and at a Y/r_e of 1.4, the 120° wedge surface experiences higher pressures than the 180° surface (fig. 4(b)). At this Y/r_e, the flat surface is very near the boattail, which results in restricting the fairing curvature and tending to block off the flow. Therefore, the region between the boattail and the flat surface acts somewhat as a base region by lowering the pressures on the fore part of the flat surface, thus decreasing the absolute value of the normal-force coefficient. The wedge surface, however, is bent away from the boattail and is not as able to block off the flow around it, so less of a base region is present. At a Y/r_e of 2.03, the expected trend again is observed except at the low pressure ratios. Fairings tended to increase the amount the net interference effects repelled the 120° wedge surface and shifted the center of pressure towards the nozzle exit, as can

be seen by comparing figures 4(b) and (a). The increased pressures on the surface due to these streamlined fairings are probably caused by shocks emanating from this type fairing in addition to those originating at the boattail.

With fairings present, the pressure ratio was first increased (open symbols, fig. 4(b)) and then decreased (flagged symbols) to note any hysteresis. There appeared to be little hysteresis for the wedge-type and convex-type surfaces. This is in agreement with the data of reference 6 for a flat plate with a streamline fairing.

Convex-Type Surfaces

In general, increasing the radius of curvature increased the absolute value of normal-force coefficient for the convex surfaces (fig. 6). However, the normal-force coefficient did not vary directly with the radius of curvature as might be expected. It is believed that, as the radius of curvature was increased, a greater percentage of surface area was exposed to low-pressure regions outside of the area bounded by the line of intersection of the jet shocks with the surfaces. Also, because of the greater percentage of surface area being exposed to the low pressures as the radius of curvature was increased, the center-of-pressure location moved farther downstream of the nozzle exit.

Again, the presence of fairings usually tended to increase the absolute value of the normal-force coefficient and shifted the center of pressure towards the nozzle exit (fig. 6(b)).

Concave-Type Surfaces

Differences between arcs subtended by 60°- and 180°-angle concave surfaces show that the normal-force coefficient of the 180° arc is roughly twice that of the 60° arc at Y/r_e positions of both 1.4 and 2.03 (fig. 7). If the pressure distribution on the surfaces is axisymmetric and independent of arc length, simple trigonometric relations show that the normal force on a 180° arc is twice the normal force of the 60° arc. The pressure profiles of figure 8 show that the pressure distributions are approximately symmetric about the center of curvature of the concave surface.

Center-of-pressure locations (fig. 7) showed little change with arc length. This is in agreement with the pressure profiles of figure 8. As the pressure ratio was increased, the pressure profiles for each surface remained quite similar.

Extending the 180° concave surface to meet the parabolic afterbody generally increased the absolute value of the normal-force coefficient and shifted the center-of-pressure location farther downstream (fig. 9).

Pressure Fluctuations

Figure 10 presents typical pressure fluctuations at Y/r_e of 2.03 without fairings. These pressure fluctuations were believed to be caused by the turbulent mixing zone between the jet and the free stream. Amplitudes increased when changing from a wedge to a convex surface, or from a convex to a concave surface in both the fore and aft pickup locations. Although the pressure recording system was accurate to 100 cycles per second, no predominant frequencies were observed.

SUMMARY OF RESULTS

The following results were obtained from an investigation of the influence of a jet on a series of surfaces of simple contour. Data were obtained over a range of jet pressure ratios from a jet-off condition to a pressure ratio of 9 at a free-stream Mach number of 1.6:

1. Decreasing the angle of wedge-type surfaces without fairings showed that the absolute value of normal-force coefficient decreased with decreasing angle and also generally shifted the center-of-pressure location farther downstream of the nozzle exit.

2. Increasing the radius of curvature of the convex-type surfaces increased the absolute value of normal-force coefficient and generally shifted the center-of-pressure location farther downstream of the nozzle exit.

3. Changing the arc length of concave-type surfaces from 60° to 180° showed that the absolute value of the normal-force coefficient of the 180° arc was approximately twice that of the 60° arc, but showed no appreciable effect on center-of-pressure location.

4. In general, streamlined fairings tended to increase the jet repelling forces on the various contoured surfaces and shifted the center of pressure toward the nozzle exit.

Lewis Flight Propulsion Laboratory
National Advisory Committee for Aeronautics
Cleveland, Ohio, January 17, 1956

REFERENCES

1. Squire, H. B.: Jet Flow and Its Effects on Aircraft. Aircraft Eng., vol. XXII, no. 253, Mar. 1950, pp. 62-67.

2. Falk, H.: The Influence of the Jet of a Propulsion Unit on Nearby Wings. NACA TM 1104, 1946.

3. Hatch, John E., Jr., and Savelle, William M.: Some Effects of a Sonic Jet Exhaust on the Loading over a Yawed Fin at a Mach Number of 3.03. NACA RM L52L02a, 1953.

4. Potter, J. Leith, and Shapiro, Norman M.: Some Effects of a Propulsion Jet on the Flow over the Fins of a Missile. Rep. 2R3F, Ord. Missile Labs., Redstone Arsenal, Jan. 11, 1954. (Proj. TB3-0108.)

5. Valerino, Alfred S.: Jet Effects on Pressure Loading of All-Movable Horizontal Stabilizer. NACA RM E54C24, 1954.

6. Englert, Gerald W., Wasserbauer, Joseph R., and Whalen, Paul: Interaction of a Jet and Flat Plate Located in an Airstream. NACA RM E55G19, 1955.

7. Bressette, Walter E.: Investigation of the Jet Effects on a Flat Surface Downstream of the Exit of a Simulated Turbojet Nacelle at a Free-Stream Mach Number of 2.02. NACA RM L54E05a, 1954.

8. Bressette, Walter E., and Faget, Maxime A.: An Investigation of Jet Effects on Adjacent Surfaces. NACA RM L55E06, 1955.

9. Salmi, Reino J., and Klann, John L.: Interference Effects at Mach 1.9 on a Horizontal Tail Due to Trailing Shock Waves from an Axisymmetric Body with an Exiting Jet. NACA RM E55J13a, 1956.

10. Englert, Gerald W., Vargo, Donald J., and Cubbison, Robert W.: Effect of Jet-Nozzle-Expansion Ratio on Drag of Parabolic Afterbodies. NACA RM E54B12, 1954.

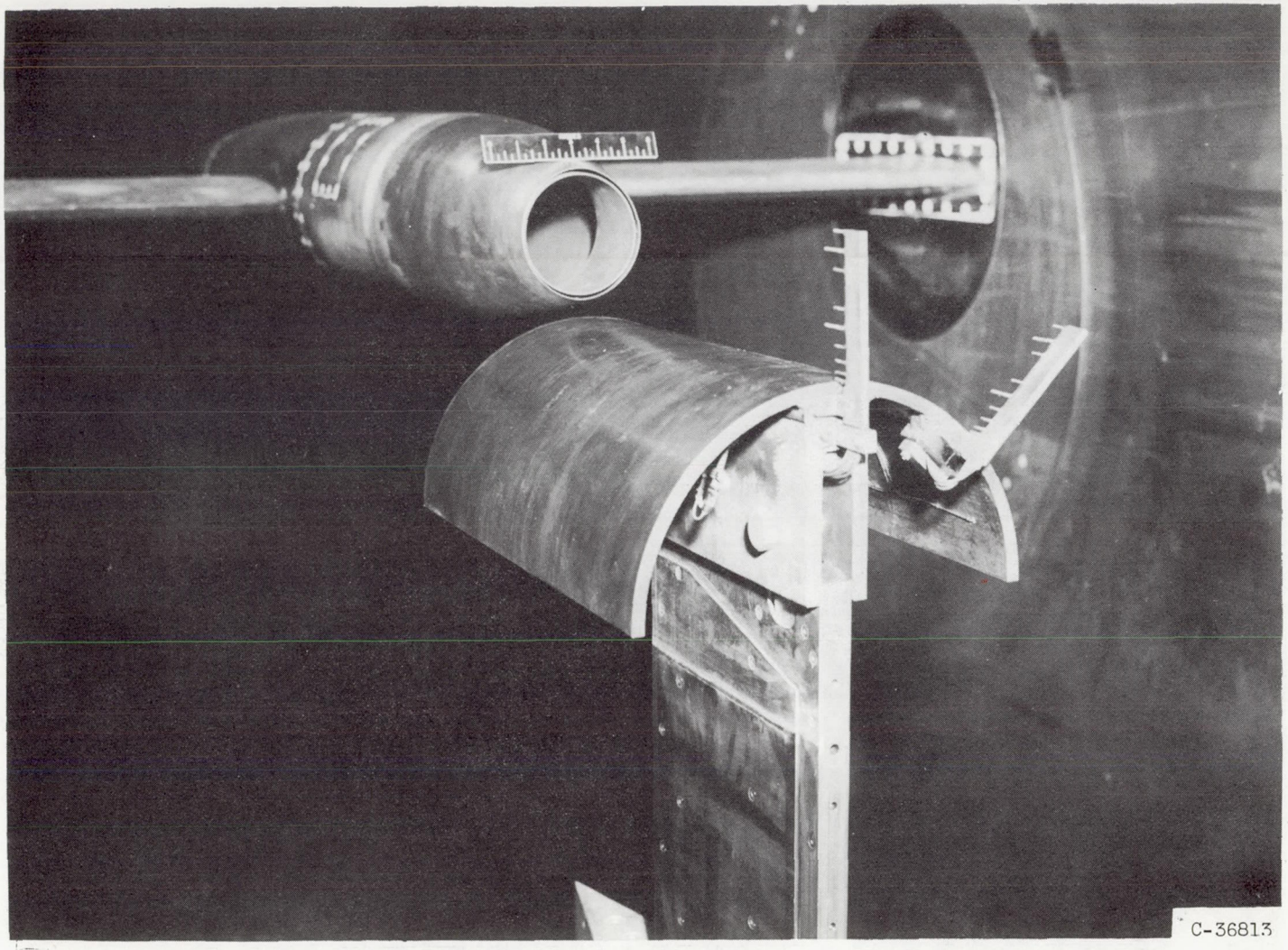

(a) Exhaust nozzle and convex surface with radius three times that of exhaust nozzle radius. No fairing present.

Figure 1. - Apparatus in 8- by 6-foot tunnel test section.

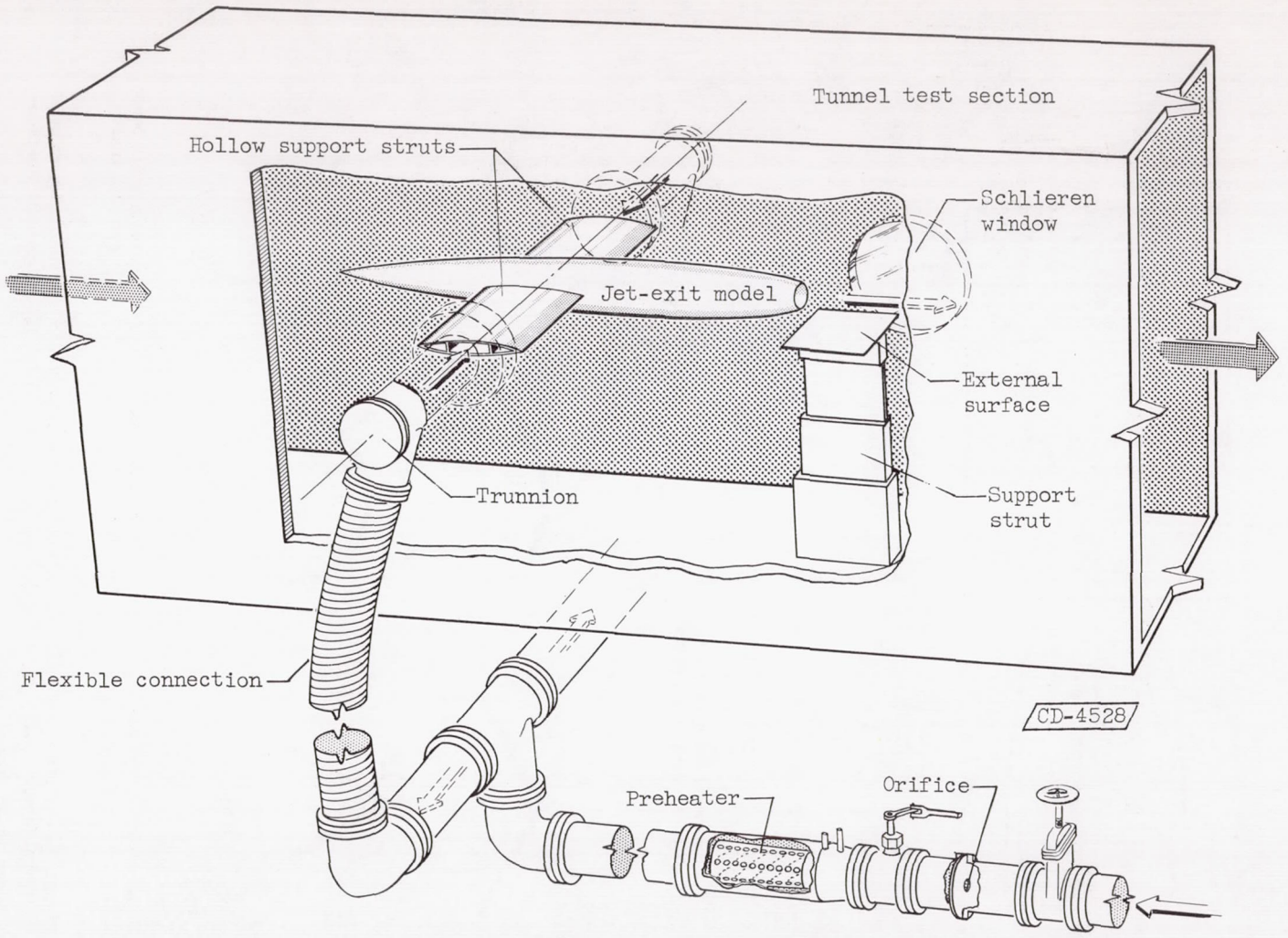

(b) Schematic drawing of interaction study model.

Figure 1. - Concluded. Apparatus in 8- by 6-foot tunnel test section.

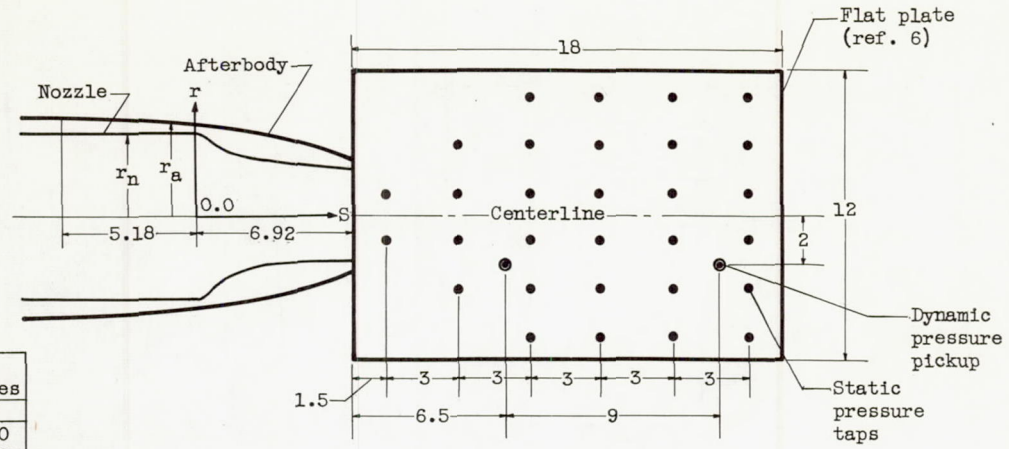

Nozzle coordinates	
S	r
0	3.50
0.35	3.495
0.71	3.410
1.04	3.215
1.38	2.985
1.73	2.715
2.07	2.550
2.42	2.390
2.76	2.280
3.11	2.190
3.56	2.139
3.81	2.089
4.15	2.060
4.84	2.035
5.52	2.032
6.23	2.030
6.92	2.030

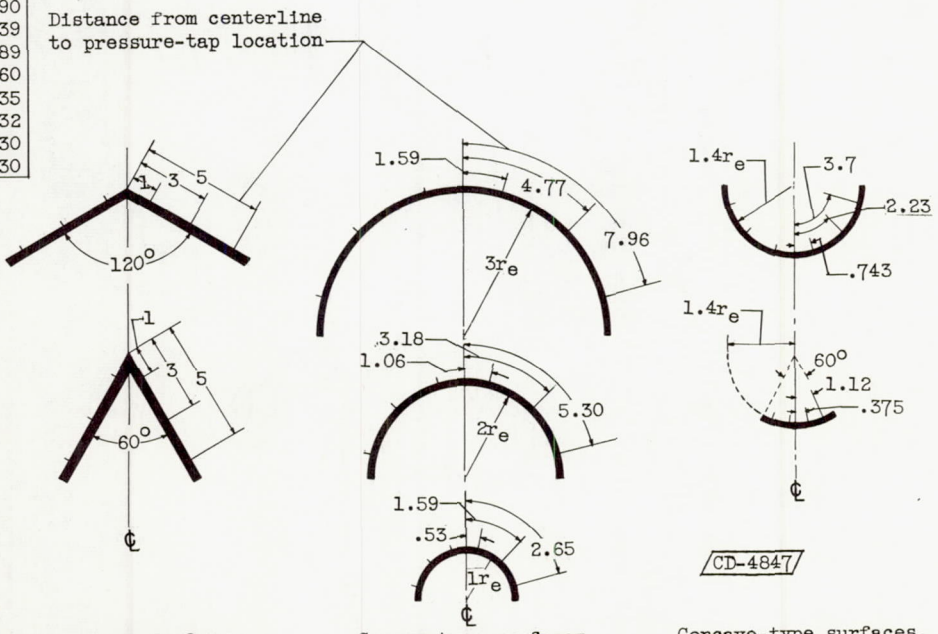

Wedge-type surfaces

Convex-type surfaces, 180° arcs

Concave-type surfaces, 180° and 60° arcs

Figure 2. - Surface and boattail details (all dimensions in inches). Equation of parabolic afterbody: $r_a = 4.125 - \frac{4.125}{(18)^2}(S \pm 5.18)^2$. Length for all surface types is 18 inches.

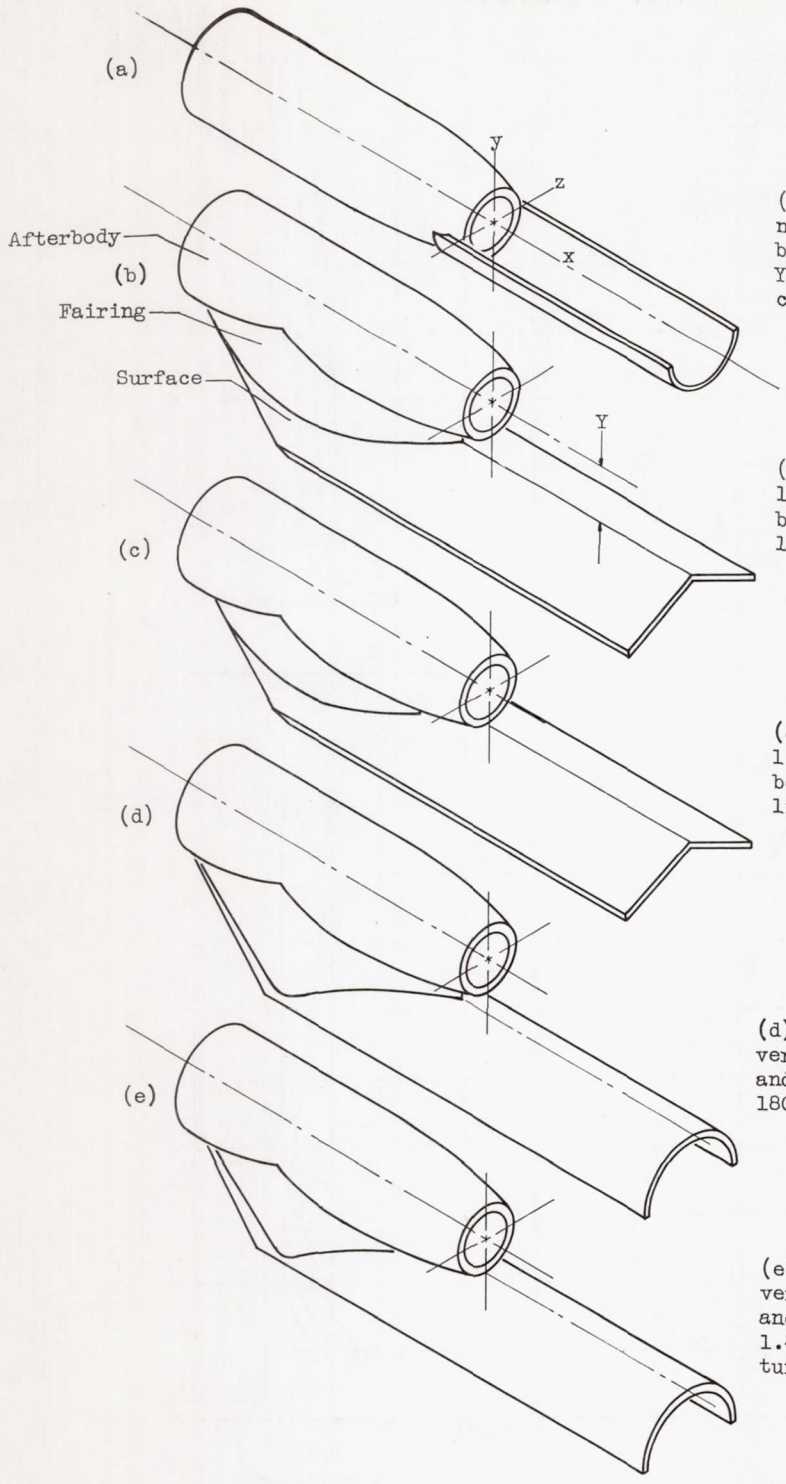

(a) Extended concave surface; no fairing; vertical distance between plate and nozzle centerline, Y/r_e, 1.4; 180° arc; radius of curvature, $1.4r_e$.

(b) Wedge surface; fairing; 120° angle; vertical distance between plate and nozzle centerline, Y/r_e, 2.03.

(c) Wedge surface; fairing; 120° angle; vertical distance between plate and nozzle centerline, Y/r_e, 1.4.

(d) Convex surface; fairing; vertical distance between plate and nozzle centerline, Y/r_e, 2.03; 180° arc; radius of curvature, $2r_e$.

(e) Convex surface; fairing; vertical distance between plate and nozzle centerline, Y/r_e, 1.4; 180° arc; radius of curvature, $2r_e$.

Figure 3. - Fairings with different type surfaces.

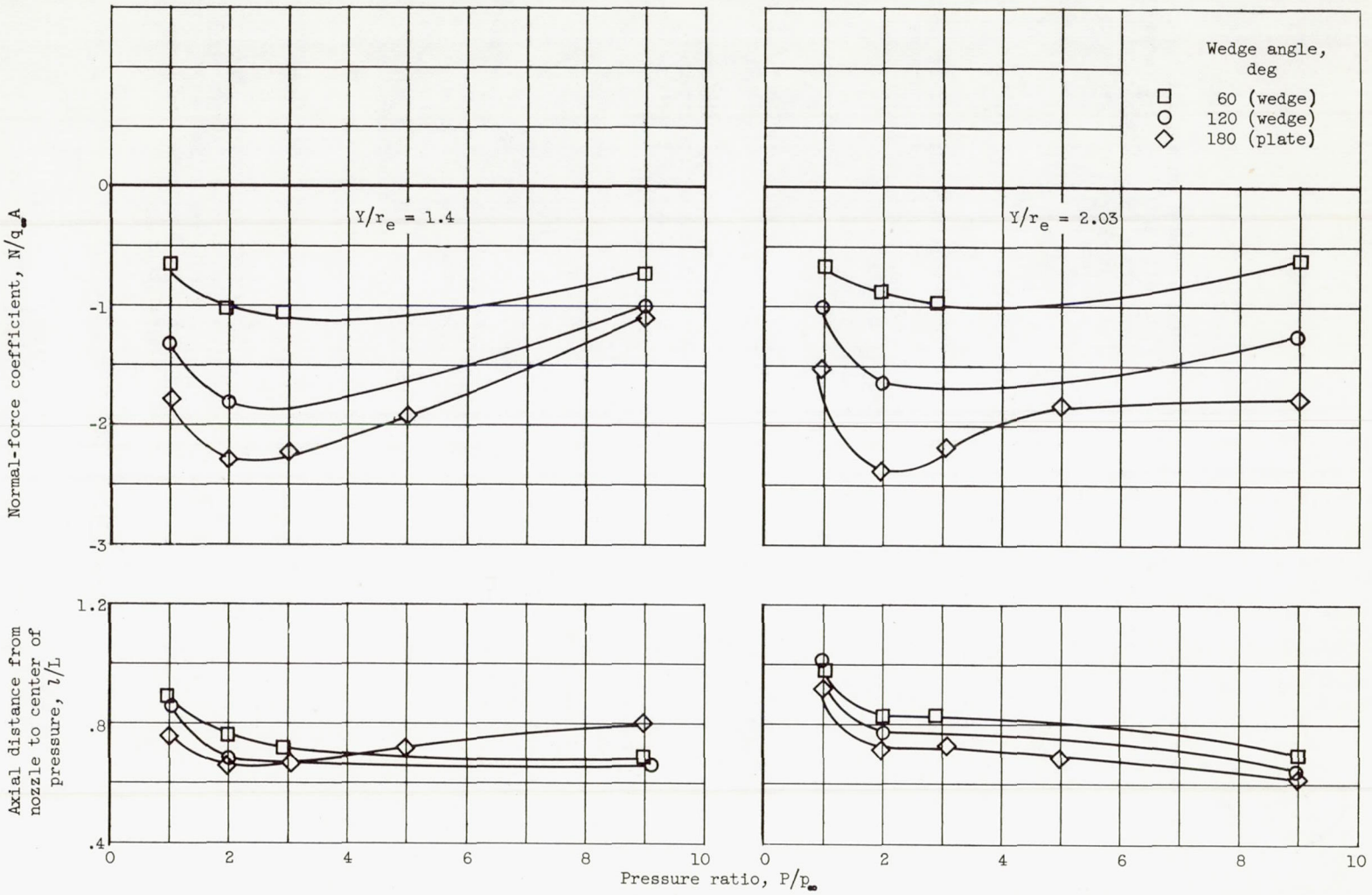

(a) Without fairings.

Figure 4. - Results of varying wedge angle.

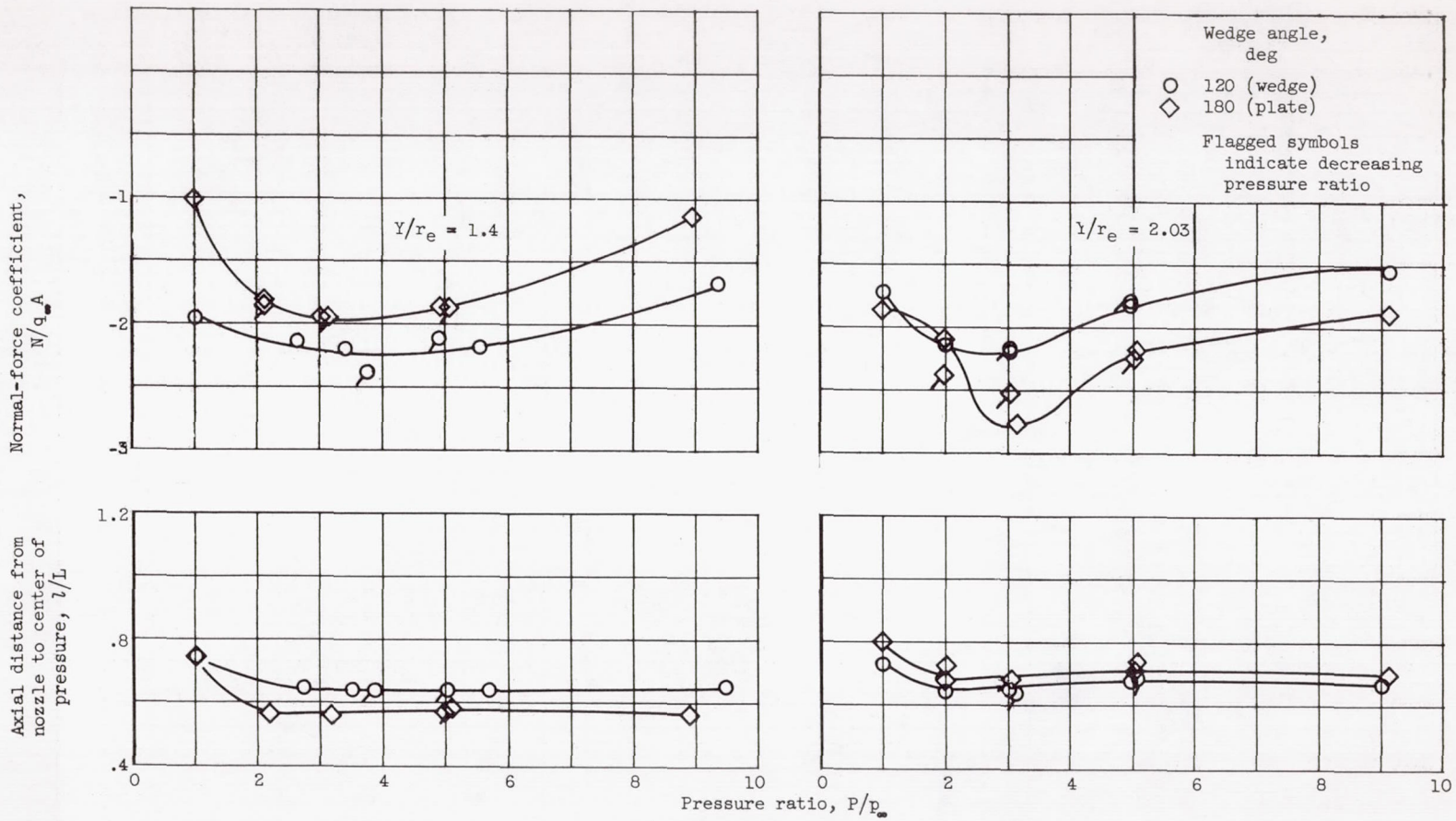

(b) With fairings.

Figure 4. - Concluded. Results of varying wedge angle.

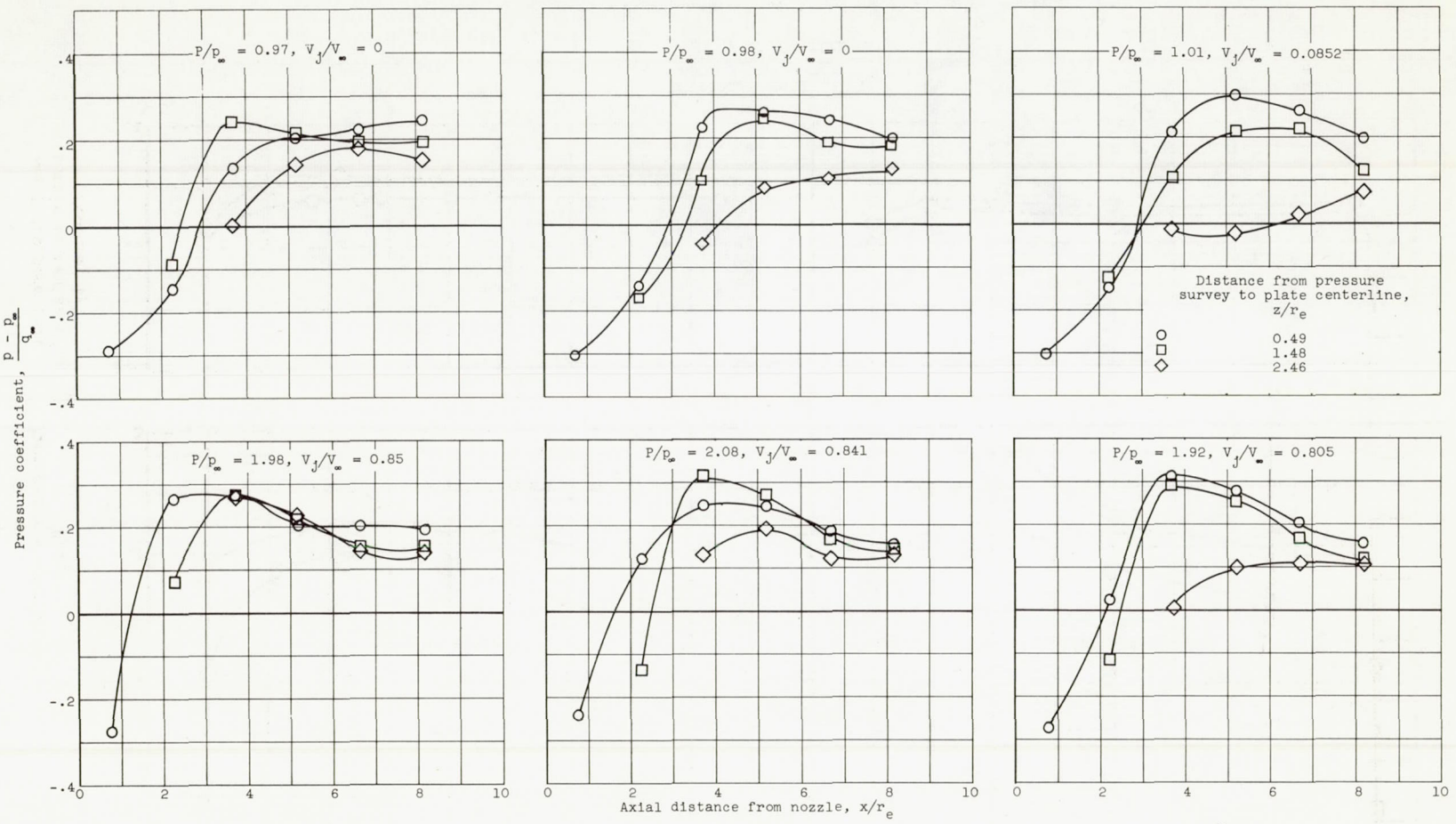

(a) 180° plate. (b) 120° wedge. (c) 60° wedge.

Figure 5. - Pressure profiles on wedge-type surfaces. Vertical distance between plate and nozzle, Y/r_e, 2.03.

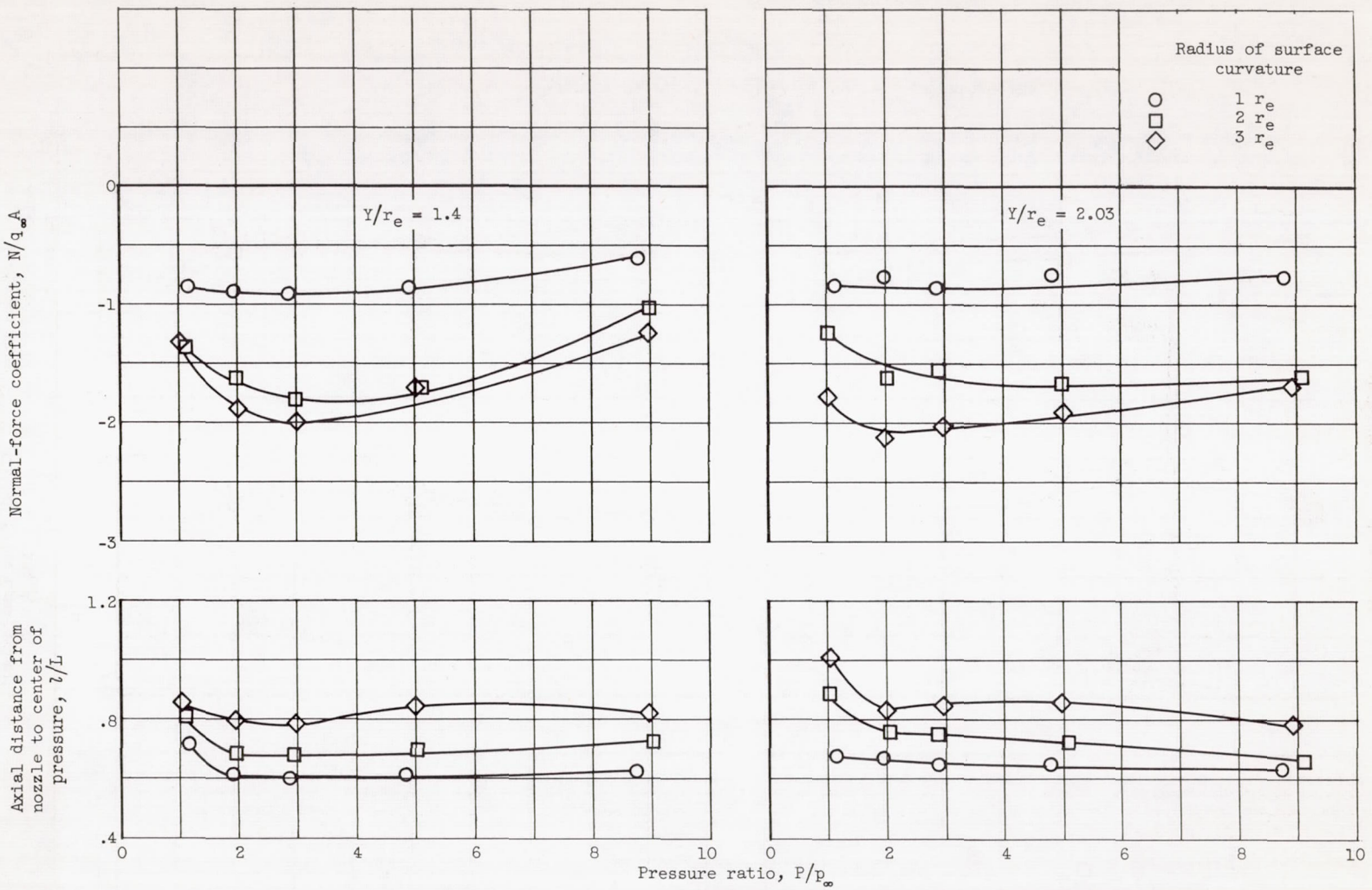

(a) Without fairings.

Figure 6. - Variation of radius of curvature of convex surface.

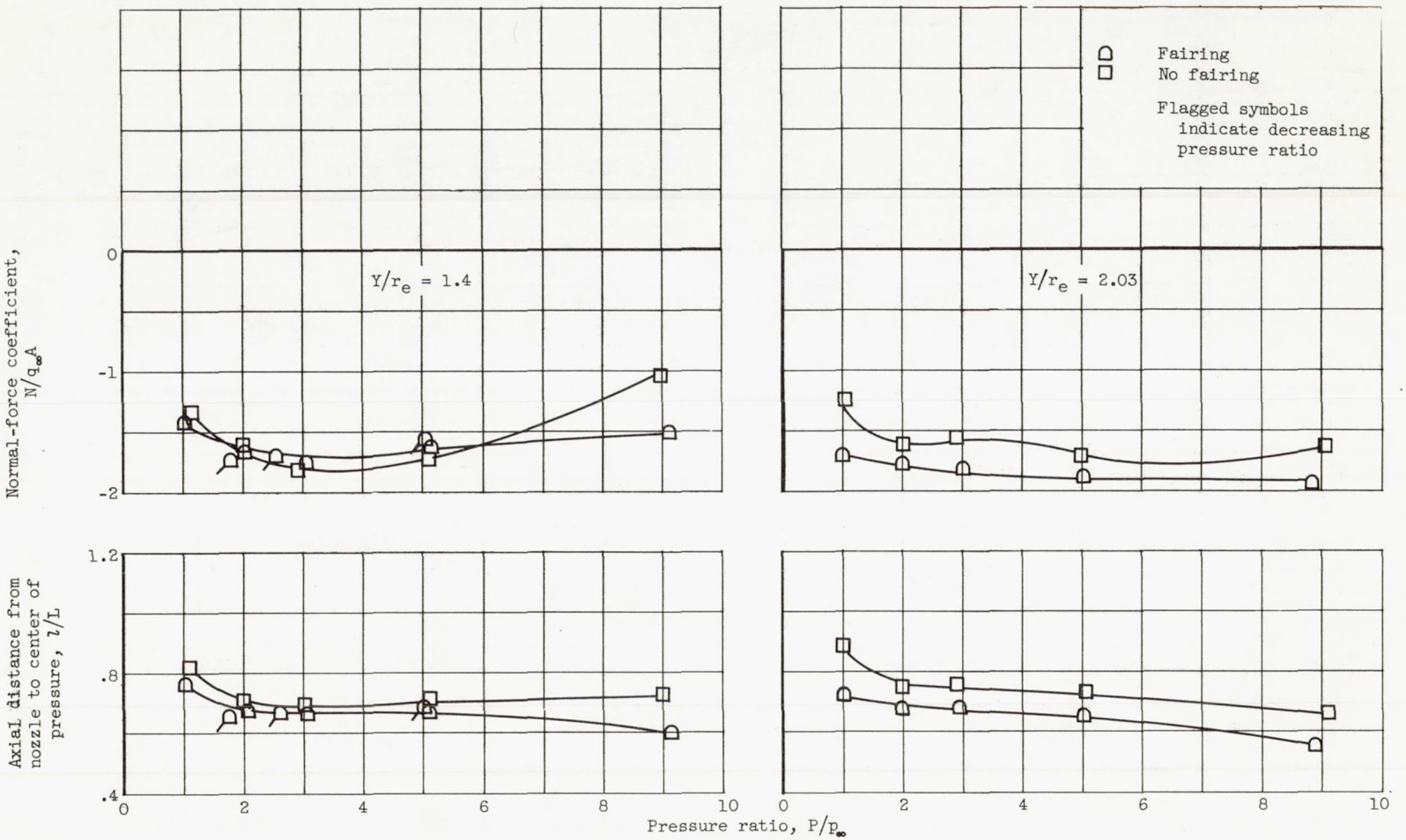

(b) With and without fairings. Radius of surface curvature, $2r_e$.

Figure 6. - Concluded. Variation of radius of curvature of convex surface.

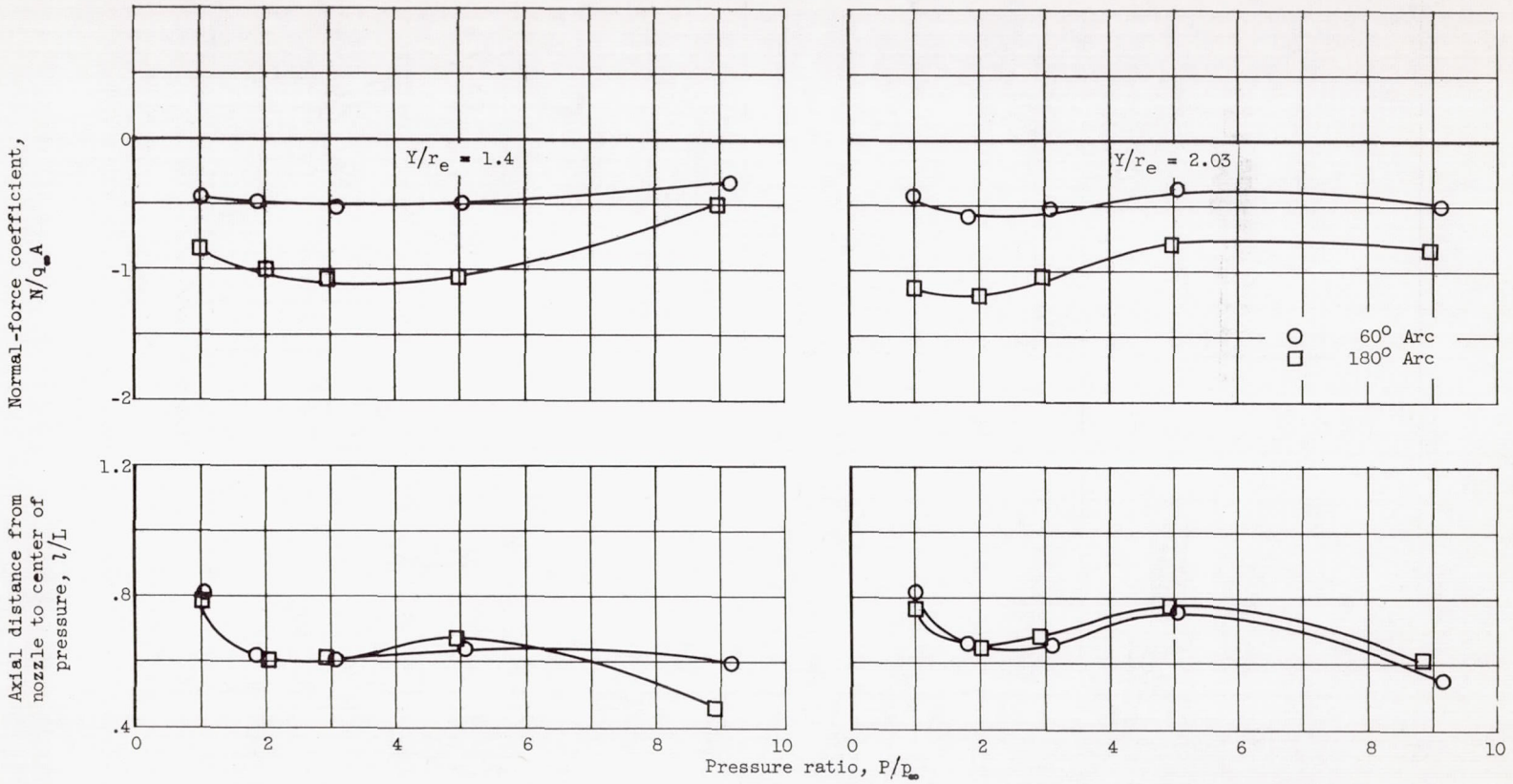

Figure 7. - Influence of arc length of concave surfaces. Without fairings; radius of surface curvature, $1.4r_e$.

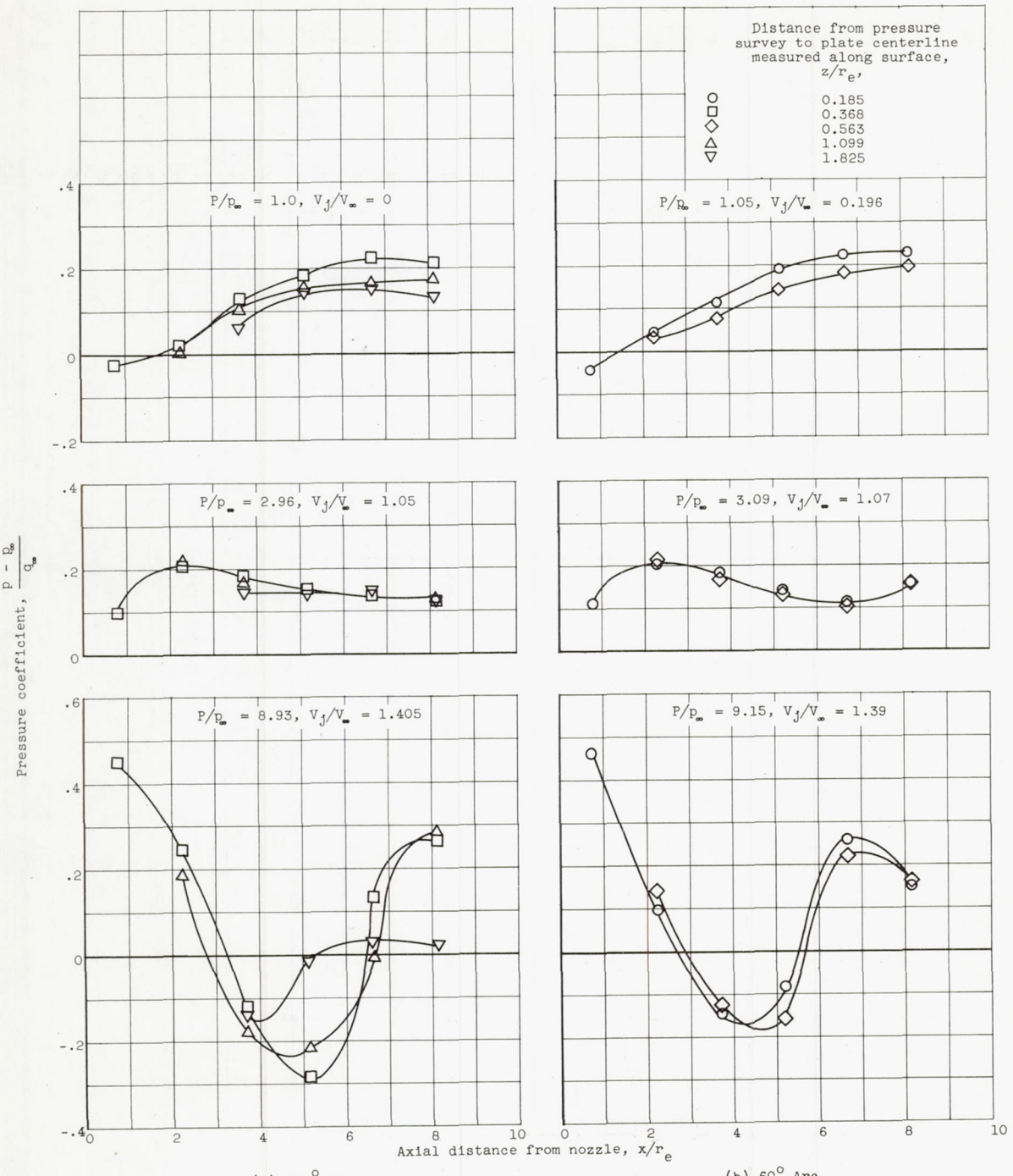

Figure 8. - Pressure profiles for concave surfaces. Vertical distance between plate and nozzle, Y/r_e, 1.4.

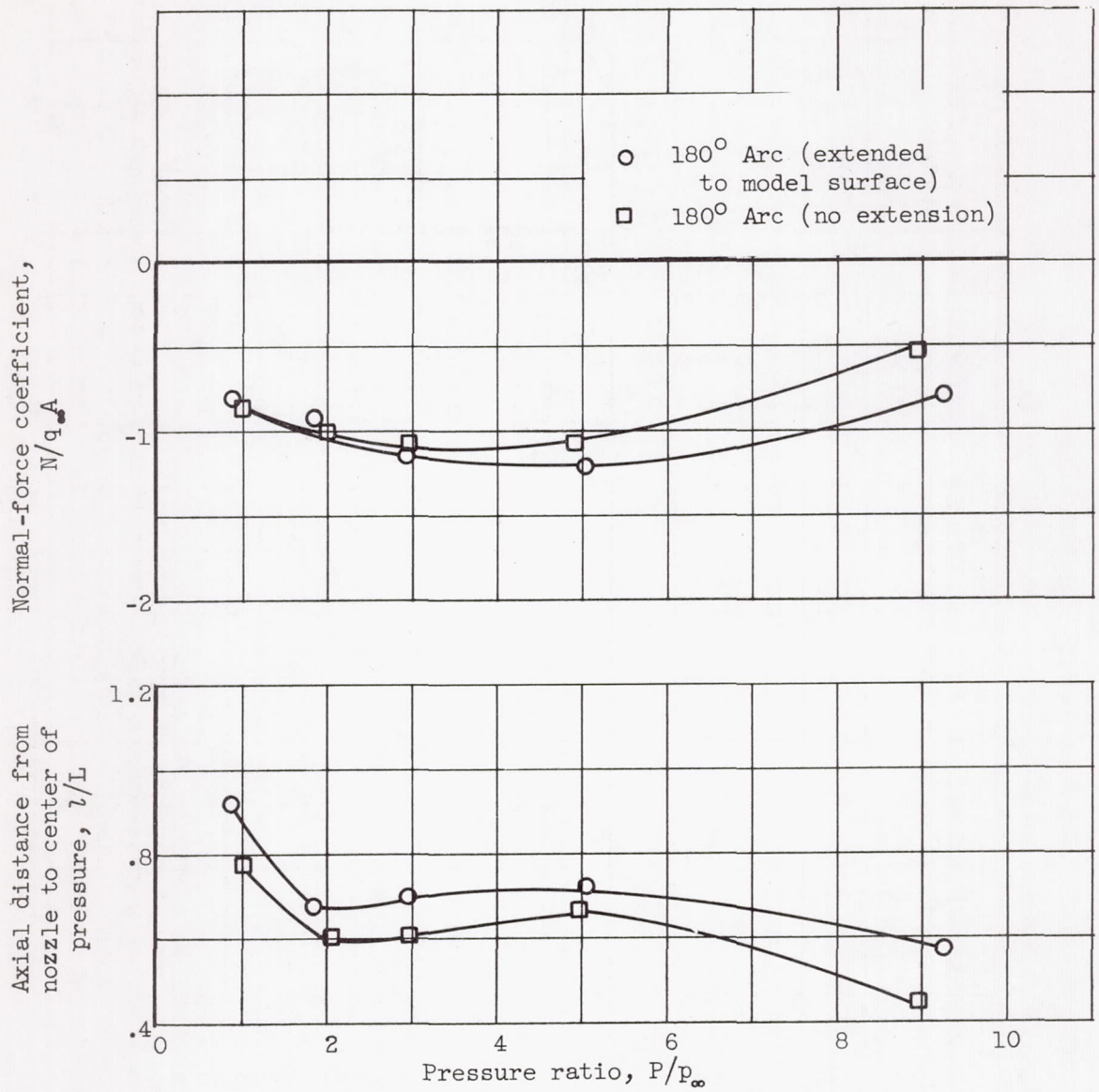

Figure 9. - Effect of extending concave surface. Mach number, 1.6; vertical distance between plate and nozzle, Y/r_e, 1.4; radius of surface curvature, $1.4r_e$.

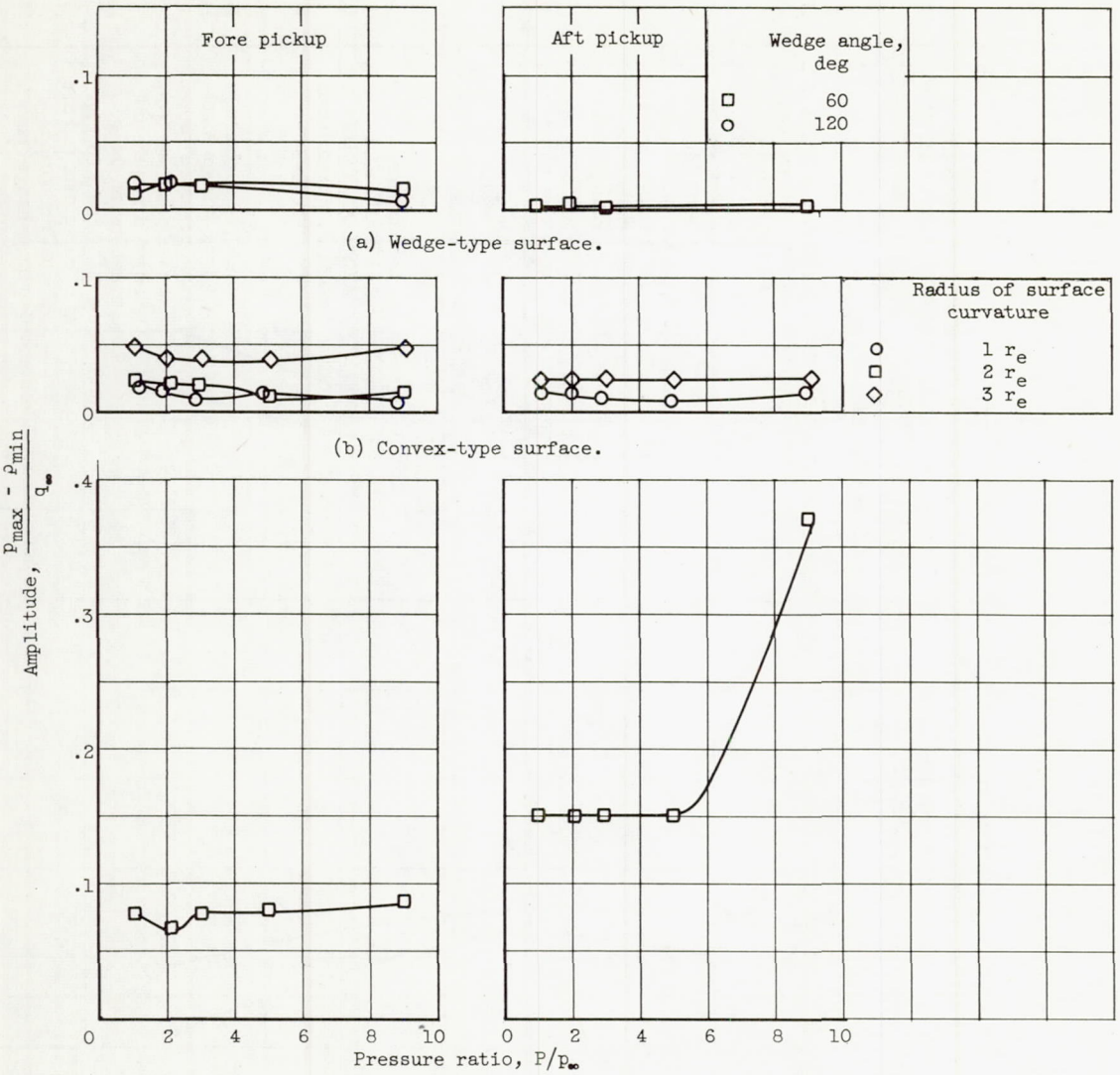

Figure 10. - Pressure fluctuations for the various type surfaces. Vertical distance between plate and nozzle, Y/r_e, 2.03; without fairings.